Solvent-Induced Electron Transfer and Electronic Delocalization in Mixed-Valence Complexes. Spectral Properties

Gregory A. Neyhart, Cliff J. Timpson, W. Douglas Bates, and Thomas J. Meyer*

Contribution from the Department of Chemistry, The University of North Carolina, Chapel Hill, North Carolina 27599-3290

Received October 23, 1995[⊗]

Abstract: Spectra of the mixed-valence complexes $[(bpy)_2ClOs(L)Ru(NH_3)_5]^{4+}$ (L = 4,4′-bipyridine, pyrazine; bpy = 2,2′-bipyridine) are highly solvent dependent. They provide oxidation state specific spectral markers which show that oxidation states for L = 4,4′-bpy are $Os^{III}-Ru^{II}$ in solvents of donor number (DN) < 14. In solvents of high donor number (DN > 15) they are $Os^{II}-Ru^{III}$. The isomers coexist at donor numbers 14−15 and the distribution between them tuned in mixtures of acetonitrile and propylene carbonate demonstrating that intramolecular electron transfer can be induced by varying the solvent. Both $Os^{III}-Ru^{II}$ and $Os^{II}-Ru^{III}$ display broad, solvent-dependent intervalence transfer (IT) bands in the near infrared (NIR). There are two isomers of $[(bpy)_2ClOs(pz)Ru(NH_3)_5]^{4+}$ as well. In one, which is dominant in solvents of DN < 22, the oxidation states are $[(bpy)_2ClOs^{III}(pz)Ru^{II}(NH_3)_5]^{4+}$. This is shown by the appearance of $d\pi \rightarrow d\pi$ marker bands for Os^{III} (at 4200 and 5800 cm^{-1} in CD_3CN), ν(bpy) Os^{III} bands in the mid-IR, and the pattern of UV−visible bands. For this isomer a narrow, structured IT band is observed at ∼8100 cm^{-1} which is nearly solvent independent in solvents of DN ≥ 11.9. The second isomer, $[(bpy)_2ClOs^{II}(pz)Ru^{III}(NH_3)_5]^{4+}$, is dominant at DN > 24. It has IT bands in the NIR which are broad and solvent dependent. It is concluded that there is significant through-pyrazine electronic coupling between Os^{III} and Ru^{II} in $[(bpy)_2ClOs^{III}(pz)Ru^{II}(NH_3)_5]^{4+}$, but localized oxidation states, and a residual solvent−vibrational barrier to intramolecular electron transfer continue to exist. The exchanging electron is in a $d\pi(Ru^{II})$ orbital largely orthogonal to the bridge. In $[(bpy)_2ClOs^{II}(pz)Ru^{III}(NH_3)_5]^{4+}$ electronic coupling is much less. Its properties are consistent with those of Class II in the Robin and Day mixed-valence classification scheme. The two isomers coexist in trimethyl phosphate (DN = 23.0) and formamide (DN = 24.0). From the temperature dependence of the mixed-valence equilibrium in trimethyl phosphate, $[(bpy)_2ClOs^{III}(pz)Ru^{II}(NH_3)_5]^{4+} \rightleftharpoons [(bpy)_2ClOs^{II}(pz)Ru^{III}(NH_3)_5]^{4+}$, K(297K) = 2.8, $\Delta H° = -8.2 \pm 2$ kcal/mol, and $\Delta S° = -27 \pm 6$ cal mol^{-1} deg^{-1}. Because of the difference in the extent of electronic delocalization between the two isomers, intramolecular electronic transfer is a complex event involving coupled electronic and nuclear motions. There is no simple relationship between optical and thermal electron transfer.

Introduction

In the previous paper, electrochemical measurements revealed two novel, solvent-based phenomena in the mixed-valence ions $[(bpy)_2ClOs(L)Ru(NH_3)_5]^{4+}$ (bpy = 2,2′-bipyridine; L = 4,4′-bipyridine (4,4′-bpy) or pyrazine (pz)).[1]

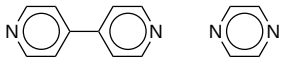

(4,4′-bpy) (pz)

The first was a solvent-induced, intramolecular electron transfer. The second was a solvent-induced change in the extent of electronic delocalization between the $Os^{III}-Ru^{II}$ and $Os^{II}-Ru^{III}$ isomers of $[(bpy)_2ClOs(pz)Ru(NH_3)_5]^{4+}$. In this paper we present the results of spectral measurements and propose models for electronic structure and intramolecular electron transfer. Some of these results have appeared in a preliminary communication.[2]

Experimental Section

Materials. The solvents nitromethane (Gold Label spectrophotometric grade), nitrobenzene (Gold Label reagent grade), and trimethyl phosphate were all obtained from Aldrich and used as received. Acetonitrile, propylene carbonate, acetone, methanol, dimethylformamide, and dimethyl sulfoxide were all obtained from Burdick and Jackson and used without further purification. Formamide (Aldrich reagent grade) was stabilized by adding two drops of 0.l M $HClO_4$ (aq) to l0 mL of the solvent immediately before use. Benzonitrile (Aldrich HPLC grade) was purified by a method adapted from Coetzee and McGuire.[3] A volume of 75 mL of the solvent was first shaken with 25 mL of silica gel and allowed to stand overnight. The solvent was decanted and distilled from P_2O_5 under reduced pressure. The middle 60% was collected. The deuterated solvents nitromethane-d_3, nitrobenzene-d_5, acetonitrile-d_3, acetone-d_6, D_2O, CH_3OD and dimethyl sulfoxide-d_6 were all obtained from Aldrich and used without further purification. $[N(n\text{-}C_4H_9)_4](PF_6)$ was prepared from $[N(n\text{-}C_4H_9)_4]Br$ and HPF_6 following the method of Calvert[4] and recrystallized three times from ethanol.

Preparations. The salts $[(bpy)_2ClOs^{II}(4,4'\text{-bpy})](PF_6)$ and $[(bpy)_2ClOs^{II}(pz)](PF_6)$ (bpy = 2,2′-bipyridine, 4,4′-bpy is 4,4′-bipyridine, and pz = pyrazine) were prepared by the methods of Kober et al.[5] The salt $[Ru(NH_3)_5(OH_2)](PF_6)_2$ was prepared by the method described by Curtis et al.[6] The salts $[(bpy)_2ClOs(L)Ru(NH_3)_5](PF_6)_3$ where L = 4,4′-bpy or pz were prepared as described previously.[1]

(a) $[(bpy)_2ClOs(L)Ru(NH_3)_5](PF_6)_4$ (L = 4,4′-bpy or pz). The mixed-valence complexes were generated electrochemically. In a typical preparation for L = 4,4′-bpy, a three-compartment cell with

⊗ Abstract published in *Advance ACS Abstracts,* April 1, 1996.

(1) Neyhart, G. A.; Hupp, J. T.; Curtis, J. C.; Timpson, C. J.; Meyer, T. J. *J. Am. Chem. Soc.* Preceding paper in this issue.
(2) Hupp, J. T.; Neyhart, G. A.; Meyer, T. J. *J. Am. Chem. Soc.* **1986**, *108,* 5349.
(3) Coetzee, J. F.; McGuire, D. K. *J. Phys. Chem.* **1963**, *67,* 1810.
(4) Calvert, J. M.; Meyer, T. *J. Inorg. Chem.* **1982**, *21,* 3978.
(5) Kober, E. M.; Caspar, J. V.; Sullivan, B. P.; Meyer, T. J. *Inorg. Chem.* **1988**, *27,* 4587.
(6) Curtis, J. C.; Sullivan, B. P.; Meyer, T. J. *Inorg. Chem.* **1983**, *22,* 224.

0002-7863/96/1518-3730$12.00/0

the compartments separated by glass frits was charged with acetonitrile 0.l M in $[N(n\text{-}C_4H_9)_4](PF_6)$. The levels were adjusted so that a minimum amount of solvent was used to cover the frits and 20 mg of $[(bpy)_2ClOs(4,4'\text{-bpy})Ru(NH_3)_5](PF_6)_3$ was added to the central compartment. The cell was of a three electrode design, with a Pt wire auxiliary electrode and a saturated calomel electrode occupying the outside compartments and a Pt gauze electrode submerged in the central sample compartment. A potential of +0.80 V vs SCE was applied with magnetic stirring until the current fell to <3% of its original value. Upon complete oxidation to $Os^{III}-Ru^{III}$, the orange solution was removed by pipet. Another 20 mg of the fully reduced $Os^{II}-Ru^{II}$ complex was added to this solution to generate the mixed-valence complex. The solution was allowed to stir for 1 min and added dropwise into 75 mL of stirring CH_2Cl_2 which resulted in precipitation of the PF_6^- salt. The dark purple precipitate was collected on a fine glass frit, washed with several l0-mL portions of CH_2Cl_2, and dried overnight in vacuo. For L = pz, the electrolysis was carried out at +0.60 V which gave the mixed-valence complex directly. It was isolated by dropwise addition of the electrolysis solution into CH_2Cl_2. Yields were essentially quantitative in either case.

(b) $[(NH_3)_5Ru(L)](PF_6)_2$ (L = 4,4′-bpy or pz). A quantity of 50 mg of $[Ru(NH_3)_5(OH_2)](PF_6)_2$ and a 20-fold excess of ligand L were placed in a 50-mL Erlenmeyer flask. The flask was fitted with a rubber septum and purged with Argon through syringe needles for 30 min. A volume of l0 mL of Argon-deaerated acetone was added by syringe and the mixture was stirred at room temperature in the absence of light under a constant Argon purge for 30 min. The salt $[(NH_3)_5Ru(L)](PF_6)_2$ was precipitated by dropwise addition of the reaction mixture to 200 mL of stirring diethyl ether. The precipitate was collected by filtration on a fine glass frit and washed with large amounts of diethyl ether to remove any excess ligand. The purity of the complex was judged by cyclic voltammetry.

Measurements. UV−visible spectra were recorded by using either Bausch and Lomb 2000 or Hewlett-Packard Model 845lA diode array spectrophotometers. Near-infrared spectra were recorded by using a Cary Model l7I spectrophotometer. Controlled potential electrolysis was performed by using a Princeton Applied Research Model l73 potentiostat and cyclic voltammetry by using a Princeton Applied Research Model l75 universal programmer as a potential sweep generator. Current vs time and current vs applied potential traces were recorded on a Hewlett-Packard Model 70l5B X−Y recorder. Variable temperature spectra were obtained by using an Oxford Instruments DN1704 liquid nitrogen dewar and No. 3120 temperature controller in the sample compartment of a Cary 14 spectrophotometer modified by On Line Instrument Sytems (OLIS) of Bogart, Georgia. Spectra were acquired by using software developed by OLIS. The reference cell was at room temperature. Solvent versus solvent baselines were recorded at each temperature for baseline subtraction. Infrared spectra were acquired on a Mattson Instruments Galaxy 5000 Fourier-transform infrared (FT-IR) spectrophotometer supported by MacFirst version 7.0.2b software.

Results

UV−Visible Spectra. Near-UV, visible spectra of $[(bpy)_2ClOs^{II}(L)Ru^{II}(NH_3)_5]^{3+}$ (L = pz, 4,4′-bpy) consist of a series of overlapping $d\pi(Os^{II}) \rightarrow \pi^*(L)$, $\pi^*(bpy)$, and $d\pi(Ru^{II}) \rightarrow \pi^*(L)$ bands which are solvent dependent (Table 1, supporting information) because of their charge transfer character. The largest shifts with solvent are observed for $d\pi(Ru^{II}) \rightarrow \pi^*(L)$ with λ_{max} for $[(bpy)_2ClOs^{II}(4,4'\text{-bpy})Ru^{II}(NH_3)_5]^{3+}$ increasing from 515 nm in nitromethane to 599 nm in dimethyl sulfoxide. Representative spectra have been published.[2]

Spectra of the mixed-valence ions $[(bpy)_2ClOs(L)Ru(NH_3)_5]^{4+}$ are also solvent dependent. In addition to spectral shifts, there is evidence for solvent induced changes in oxidation state. For $[(bpy)_2ClOs(4,4'\text{-bpy})Ru(NH_3)_5]^{4+}$ in nitromethane, Figure 1, the oxidation states are $Os^{III}-Ru^{II}$ as shown by the absence of $d\pi(Os^{II}) \rightarrow \pi^*$(bpy, 4,4′-bpy) bands at 420 and 700 nm. In dimethylformamide it is $Os^{II}-Ru^{III}$ as shown by the absence of $d\pi(Ru^{II}) \rightarrow \pi^*(4,4'\text{-bpy})$.

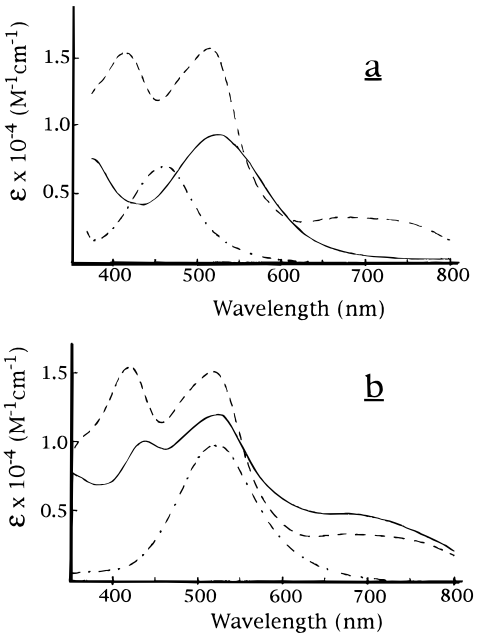

Figure 1. Visible spectra of $[(bpy)_2ClOs(4,4'\text{-bpy})Ru(NH_3)_5]^{4+}$ (—), $[(bpy)_2ClOs^{II}(4,4'\text{-bpy})]^+$ (— —), and $[(NH_3)_5Ru^{II}(4,4'\text{-bpy})]^{2+}$ (— · —): (a) in nitromethane, where the oxidation states in the mixed-valence ion are $Os^{III}-Ru^{II}$, and (b) in dimethylformamide, where they are $Os^{II}-Ru^{III}$.

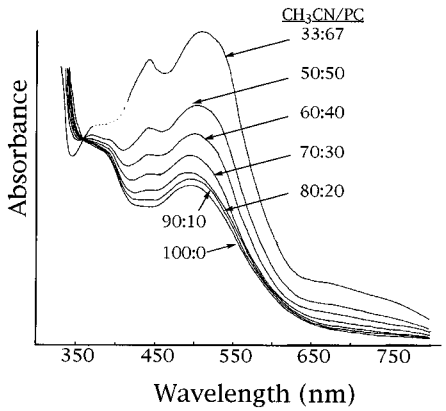

Figure 2. Visible spectra of $[(bpy)_2ClOs(4,4'\text{-bpy})Ru(NH_3)_5]^{4+}$ in acetonitrile/propylene carbonate (PC) mixtures at the volume percents indicated. The solutions contained a 30% excess of $Os^{III}-Ru^{III}$ to supress disproportionation.

As shown in the previous paper, the interconversion between oxidation states is caused by the difference in solvent dependences for the $Os^{III/II}$ and $Ru^{III/II}$ couples. Potentials for the $Ru^{III/II}$ couple vary with the solvent donor number (DN, the heat released in kcal/mol when adduct formation occurs between the solvent and the electron pair acceptor $SbCl_5$ in 1,2-dichloroethane.[7])

The transition between oxidation states for L = 4,4′-bpy occurs near DN = 14. This donor number region was explored in more detail by using mixtures of acetonitrile (DN = 14.1) and propylene carbonate (DN = 15.1), Figure 2. Similarly, UV−visible spectra of $[(bpy)_2ClOs(pz)Ru(NH_3)_5]^{4+}$ (Figure 3, Table 2, supporting information) reveal that a crossover occurs between methanol (DN = 19.0) and trimethyl phosphate (DN = 23.0).

(7) (a) Gutmann, V. *The Donor−Acceptor Approach to Molecular Interactions*; Plenum Press: New York, 1978. (b) Gutmann, V. *Electrochim. Acta* **1976**, *21*, 661. (c) Gutmann, V. *Coordination Chemistry in Non-Aqueous Solutions*; Springer-Verlag: New York, 1968. (d) Sawyer, D. T.; Roberts, J. L. *Experimental Electrochemistry for Chemists*; John Wiley and Sons: New York, 1974.

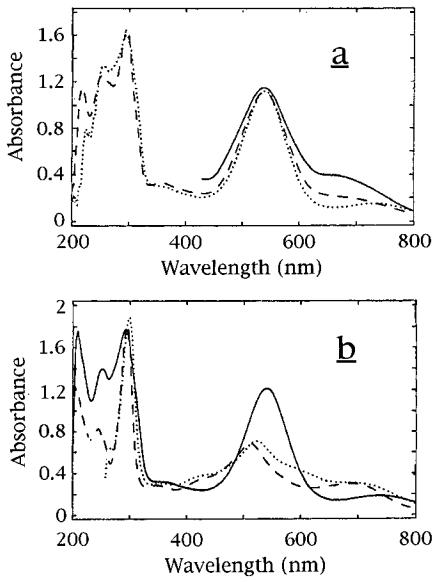

Figure 3. UV−visible spectra of $[(bpy)_2ClOs(pz)Ru(NH_3)_5]^{4+}$: (a) in nitrobenzene (—), acetonitrile (− −), or propylene carbonate (•••) and in methanol (—), trimethyl phosphate (− −), or dimethyl sulfoxide (•••).

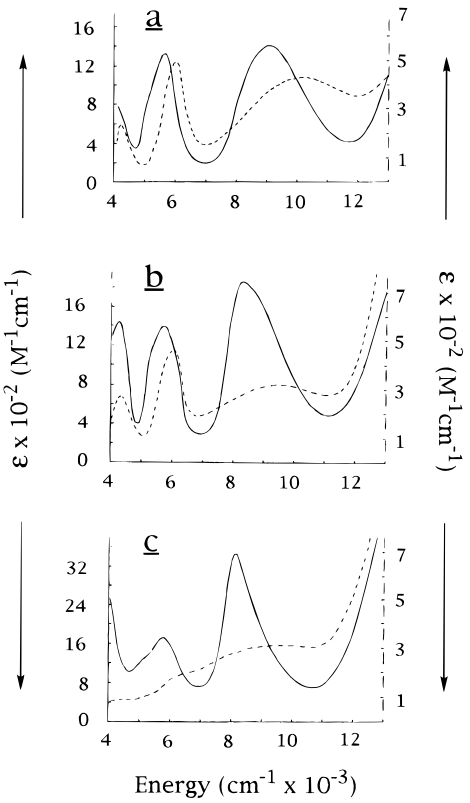

Figure 4. Near-infrared spectra of $[(bpy)_2ClOs(L)Ru(NH_3)_5]^{4+}$ where L = pz (—, left-hand axis) or 4,4′-bpy (− −, right-hand axis) in (a) nitromethane-d_3, (b) acetonitrile-d_3, or (c) acetone-d_6.

Near-Infrared (NIR) Spectra. Representative NIR spectra for the mixed-valence ions are shown in Figures 4 and 5 and band parameters are listed in Table 1 as a function of donor number. NIR spectra of $[(bpy)_2ClOs(pz)Ru(NH_3)_5]^{4+}$ in trimethyl phosphate from 240 to 316 K are shown in Figure 6.

These spectra can be counterion and concentration dependent, especially in nonpolar solvents.[8−10] Our spectroscopic results were obtained on PF_6^- salts of the isolated complexes to minimize these effects. Within the concentration limits used, 2×10^{-4} to 2×10^{-3} M, both bandshapes and molar extinction coefficients were independent of the concentration of complex.

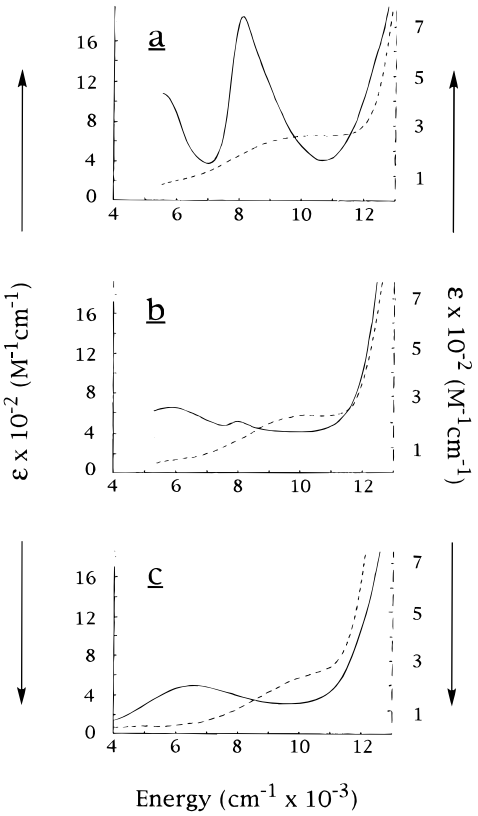

Figure 5. Near-infrared spectra of $[(bpy)_2ClOs(L)Ru(NH_3)_5]^{4+}$ where L = pz (—, left-hand axis) or 4,4′-bpy (− −, right-hand axis) in (a) D_2O, (b) formamide, or (c) dimethyl sulfoxide-d_6.

Infrared Spectra. Infrared spectra for $[(bpy)_2ClOs(pz)Ru(NH_3)_5]^{5+,4+,3+}$ (L = pz, 4,4′-bpy) in CD_3CN are shown in Figure 7. A selected listing of bands in the region 1200−1700 cm^{-1} for the three complexes and for $[(bpy)_2ClOs(pz)]^{2+/+}$ is given in Table 2. Competing absorptions by solvent limited the accessible spectral range. Spectra of the same three ions in KBr were similar with slight shifts in band energies. A complete listing of band energies in CD_3CN and KBr is given in Table 3, supporting information.

In order to search for possible low-energy bands of electronic origin, the IR measurements were extended into the NIR. There is no evidence for a new, well-defined absorption feature below 3000 cm^{-1} for $[(bpy)_2ClOs(pz)Ru(NH_3)_5]^{4+}$. Given the concentrations used in the IR experiments ($\sim 1 \times 10^{-2}$ M), an electronic band with ϵ_{max} as high as 500 M^{-1} cm^{-1} would have had an intensity of only 20% of the most intense band in the infrared.

Discussion

Of the five visible absorption bands for $[(bpy)_2ClOs^{II}(L)Ru^{II}(NH_3)_5]^{3+}$ (L = 4,4′-bpy, pz), four are only slightly solvent dependent and can be assigned to $d\pi(Os^{II}) \rightarrow \pi^*$(bpy,L) MLCT transitions.[5,11,12] The fifth is intense and highly solvent de-

(8) Lowery, M. D.; Hammack, W. S.; Drickamer, H. G.; Hendrickson, D. N. *J. Am. Chem. Soc.* **1987**, *109*, 8019.

(9) (a) Lewis, N. A.; Obeng, Y. S. *J. Am. Chem. Soc.* **1988**, *110*, 2306. (b) Lewis, N. A.; Obeng, Y. S.; Purcell, W. L. *Inorg. Chem.* **1989**, *28*, 3796.

(10) (a) Blackbourn, R. L.; Hupp, J. T. *Chem. Phys. Lett.* **1988**, *150*, 399. (b) Blackbourn, R. L.; Hupp, J. T. *J. Phys. Chem.* **1990**, *94*, 1788.

(11) Kober, E. M. Ph.D. Dissertation, University of North Carolina at Chapel Hill, 1982.

(12) Kober, E. M.; Sullivan, B. P.; Meyer, T. J. *Inorg. Chem.* **1984**, *23*, 2098.

Table 1. Near-Infrared Spectral Data for $[(bpy)_2ClOs(L)Ru(NH_3)_5]^{4+}$ (L = 4,4′-bpy, pz)

		L = 4,4′-bpy			L = pz		
solvent	donor no.	E_{op} ($cm^{-1} \times 10^{-3}$)	ϵ ($M^{-1}\,cm^{-1}$)	$\Delta\bar{\nu}_{1/2}$ ($cm^{-1} \times 10^{-3}$)	E_{op} ($cm^{-1} \times 10^{-3}$)	ϵ ($M^{-1}\,cm^{-1}$)	$\Delta\bar{\nu}_{1/2}$ ($cm^{-1} \times 10^{-3}$)
nitromethane-d_3	2.7	10.2	430	3.54	9.03	1390	2.21
		6.01	490	0.88	5.62	1300	0.98
		4.30	240				
nitrobenzene-d_5	4.4	10.4	260	3.80	8.75	1420	2.33
		6.01	350	0.88	5.53	1120	1.18
		4.26	150				
benzonitrile	11.9	8.19	250		8.17	1690	1.61
acetonitrile-d_3	14.1	9.48	320	3.42	8.30	1850	1.85
		6.07	450	0.87	5.77	1400	1.24
		4.25	270		4.17	1430	
propylene carbonate	15.1	8.51	250		8.12	1850	1.31
acetone-d_6	17.0	9.16	300	6.10	8.10	3300	1.14
					5.78	1700	1.04
D_2O	18.0	10.31	260	6.10	8.08	1840	1.34
methanol-d	19.0	10.0[a]	340		8.15	1180	1.32
trimethyl phosphate	23.0	9.76	225	4.90	8.06	980	
					8.02	520	
formamide	24.0	10.15	230	4.82	5.90	630	
dimethylformamide	26.6	10.1[a]	250	4.64	< 6.20	750	
dimethyl sulfoxide-d_6	29.9	10.5[a]	240		6.60	480	3.80

[a] Band appears as a shoulder.

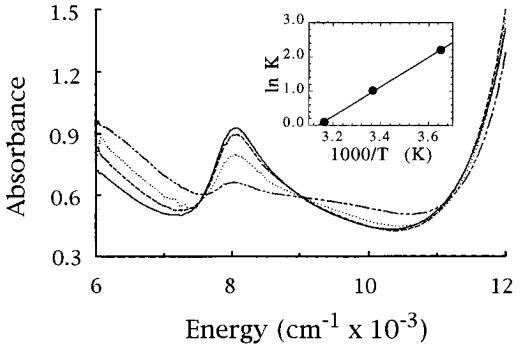

Figure 6. Near-infrared spectra of $[(bpy)_2ClOs(pz)Ru(NH_3)_5]^{4+}$ in trimethyl phosphate at 316 (—), 297 (– –), 274 (•••), and 240 K (– - -–). Inset is a plot of ln K versus $1/T$ in the temperature range 274−316 K.

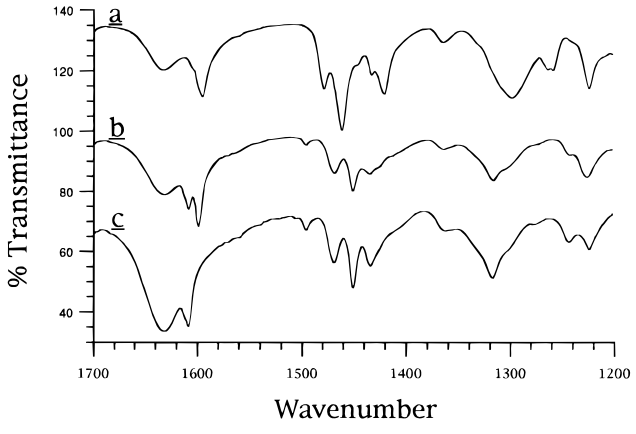

Figure 7. Infrared spectra of (a) $[(bpy)_2ClOs(pz)Ru(NH_3)_5]^{3+}$, (b) $[(bpy)_2ClOs(pz)Ru(NH_3)_5]^{4+}$, and (c) $[(bpy)_2ClOs(pz)Ru(NH_3)_5]^{5+}$ in CD_3CN.

pendent and arises from overlapping $d\pi(Os^{II},Ru^{II}) \rightarrow \pi^*(L)$ transitions. Solvatochromism in $[Ru(NH_3)_5(L)]^{2+}$ complexes is well-known.[6]

The spectral changes that occur for $[(bpy)_2ClOs(4,4'\text{-bpy})Ru(NH_3)_5]^{4+}$ between low and high donor number solvents can be explained by a change from $Os^{III}-Ru^{II}$ to $Os^{II}-Ru^{III}$. This ion is $[(bpy)_2ClOs^{III}(4,4'\text{-bpy})Ru^{II}(NH_3)_5]^{4+}$ in nitromethane (DN = 2.7) as shown by the absence of $d\pi(Os^{II}) \rightarrow \pi^*(bpy)$ bands in the visible and the appearance of $d\pi(Os^{III}) \rightarrow \pi^*(bpy)$ at ∼380 nm[11] and $d\pi(Ru^{II}) \rightarrow \pi^*(4,4'\text{-bpy})$ at 515 nm. The ion is $[(bpy)_2ClOs^{II}(4,4'\text{-bpy})Ru^{III}(NH_3)_5]^{4+}$ in dimethylformamide (DN = 26.6) where $d\pi(Os^{II}) \rightarrow \pi^*(bpy)$ bands appear at 430 and 680 nm, $d\pi(Ru^{II}) \rightarrow \pi^*(4,4'\text{-bpy})$ is lost, and a bpy-localized $\pi \rightarrow \pi^*$ band appears at 298 nm.[6,11]

These results show that the equilibrium in eq 1 is solvent dependent, consistent with the electrochemical results in the previous paper.[1]

$$[(bpy)_2ClOs^{III}(4,4'\text{-bpy})Ru^{II}(NH_3)_5]^{4+} \rightleftharpoons [(bpy)_2ClOs^{II}(4,4'\text{-bpy})Ru^{III}(NH_3)_5]^{4+} \quad (1)$$

The two isomers are present in comparable amounts ($K \sim 1$) near donor number l4.5 as shown by the the spectral variations in acetonitrile (DN = 14.1)/propylene carbonate (DN = l5.l) mixtures. From the point of steepest slope in a plot of A(430 nm) vs percent propylene carbonate, $Os^{III}-Ru^{II}$ and $Os^{II}-Ru^{III}$ are present in equal amount at ∼55% acetonitrile−45% propylene carbonate (v:v).

Similar spectral changes occur for $[(bpy)_2ClOs(pz)Ru(NH_3)_5]^{4+}$ but the switch from $Os^{III}-Ru^{II}$ to $Os^{II}-Ru^{III}$ occurs at DN = 23 (trimethyl phosphate). In $[(bpy)_2ClOs^{III}(pz)Ru^{II}(NH_3)_5]^{4+}$ the $d\pi(Ru^{II}) \rightarrow \pi^*(pz)$ band at ∼540 ± 3 nm is nearly solvent independent and yet $d\pi \rightarrow \pi^*(L)$ bands in $[Ru(NH_3)_5(L)]^{2+}$ complexes are typically highly solvent dependent.[6] A new, solvent-dependent band does appear at ∼700 nm. This is a region where $d\pi(Os^{II}) \rightarrow \pi^*(bpy)$ bands are typically found.[5,11,12] It may originate from a remote, $d\pi((NH_3)_5Ru^{II}) \rightarrow \pi^*(bpy)$ transition, eq 2. Related transitions have been identified in cyano-bridged complexes of Os and Ru.[13]

$$[(bpy)_2ClOs^{III}(pz)Ru^{II}(NH_3)_5]^{4+} \xrightarrow{h\nu} [(bpy)(bpy)^{\bullet-}ClOs^{III}(pz)Ru^{III}(NH_3)_5]^{4+} \quad (2)$$

For $[(bpy)_2ClOs^{II}(pz)Ru^{III}(NH_3)_5]^{4+}$ the expected pattern of $Os^{II} \rightarrow \pi^*(bpy,pz)$ bands appears in solvents of DN ≥ 23. The

(13) (a) Bignozzi, C. A.; Paradisi, C.; Ruffia, S.; Scandola, F. *Inorg. Chem.* **1988**, *27*, 408. (b) Schoonover, J. R.; Timpson, C. J.; Meyer, T. J.; Bignozzi, C. A. *Inorg. Chem.* **1992**, *31*, 3185.

Table 2. Infrared Band Energies (in cm^{-1}) for $[Os(bpy)_2(pz)Cl]^{2+/+}$ and $[(bpy)_2ClOs(pz)Ru(NH_3)_5]^{5+/4+/3+}$ in CD_3CN at 298 K[a]

$[(bpy)_2ClOs(pz)]^+$	$[(bpy)_2ClOs(pz)]^{2+}$	$[(bpy)_2ClOs(pz)Ru(NH_3)_5]^{3+}$	$[(bpy)_2ClOs(pz)Ru(NH_3)_5]^{4+}$	$[(bpy)_2ClOs(pz)Ru(NH_3)_5]^{5+}$
1259 s	1244 s	1259 m	1244 w	1244 w
1263 s			1264 m	
1312 w	1318 s	1299 s	1317 s	1318 s
1320 w				
1420 s	1420 s	1421 s	1435 m	1434 m
1446 w	1451 s	1433 w	1451 w	1451 s
1462 s	1469 s	1461 s	1469 s	1469 s
1480 m	1496 m	1479 m	1496 w	1496 m
1505 w	1517 w			
1584 s	1596 w	1595 s	1599 s	
1605 w	1609 s		1608 m	1608 m

[a] s, m, and w, are abbreviations for strong, medium, and weak.

Scheme 1

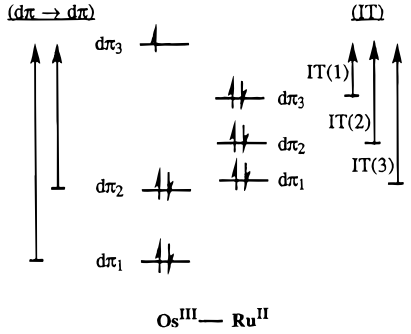

Scheme 2

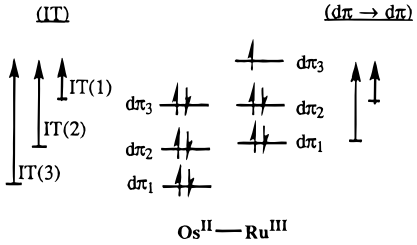

energy of $d\pi(Os^{II}) \rightarrow \pi^*(pz)$ at 500−550 nm is solvent dependent but decreased in intensity by $\sim^1/_2$.

Electronic Structure. $[(bpy)_2ClOs(4,4'\text{-}bpy)Ru(NH_3)_5]^{4+}$. NIR spectra of $[(bpy)_2ClOs(4,4'\text{-}bpy)Ru(NH_3)_5]^{4+}$ are consistent with $Os^{III}-Ru^{II}$ at DN < 14 and $Os^{II}-Ru^{III}$ at DN > 15. NIR bands arise either from intervalence transfer (IT) or interconfigurational ($d\pi \rightarrow d\pi$) transitions within the $(d\pi)^5$ core at Os^{III}, Scheme 1.[11,14,15] The IT bands are broad since their widths and energies depend on the solvent reorganizational energy. For $[(bpy)_2ClOs^{III}(4,4'\text{-}bpy)Ru^{II}(NH_3)_5]^{4+}$, a single IT band is observed which is a convolution of bands arising from three transitions, $d\pi_n(Ru^{II}) \rightarrow d\pi_3(Os^{III})$ ($n = 1, 2, 3$), Scheme 1. The $d\pi \rightarrow d\pi$ bands are narrow and solvent independent. They appear at 4000−6000 cm^{-1} as in $[(bpy)_2ClOs^{III}(py)]^{2+}$,[11] but are masked in some solvents by solvent vibrational overtones. They provide a convenient oxidation state marker for Os^{III} and verify the oxidation state distribution $Os^{III}-Ru^{II}$ (DN < 14).

For $[(bpy)_2ClOs^{II}(4,4'\text{-}bpy)Ru^{III}(NH_3)_5]^{4+}$ only the lowest of three IT bands, $d\pi_3(Os^{II}) \rightarrow d\pi_3(Ru^{III})$, Scheme 2, is observed. The higher energy bands, IT(2) and IT(3) in Scheme 2, are expected to appear ~4000 and ~6000 cm^{-1} to higher energy and are masked by more intense $d\pi(Os^{II}) \rightarrow \pi^*(bpy,4,4'\text{-}bpy)$ bands. They have been observed in other mixed-valence ions.[13b,15a] Because of the decrease in spin−orbit coupling between Ru^{III} (~1250 cm^{-1}) and Os^{III} (~3000 cm^{-1}),[16] $d\pi \rightarrow d\pi(Ru^{III})$ bands are of low intensity and fall in the infrared where they are masked by the usual infrared bands.[17]

$[(bpy)_2ClOs(pz)Ru(NH_3)_5]^{4+}$. For $[(bpy)_2ClOs^{II}(pz)Ru^{III}(NH_3)_5]^{4+}$ $d\pi(Os^{II}) \rightarrow \pi^*(bpy)$ oxidation state markers appear in the visible. IT(1) in Scheme 2 appears at 6600 cm^{-1} in DMSO-d_6, which is at lower energy than for L = 4,4′-bpy because of the reduced bridge length.[18,19] The band is solvent dependent with $E_{max} = 5900$ cm^{-1} in formamide and ~6200 cm^{-1} in dimethylformamide. IT(2) appears as a broad absorption between 9000 and 11000 cm^{-1} in formamide and dimethylformamide. IT(3) is masked by more intense MLCT bands. There is no evidence in the spectra for significant electronic delocalization.

For $[(bpy)_2ClOs^{III}(pz)Ru^{II}(NH_3)_5]^{4+}$, the appearance of $d\pi \rightarrow d\pi(Os^{III})$ bands provides evidence for Os^{III} and the oxidation states $Os^{III}-Ru^{II}$. This conclusion is consistent with the absence of $d\pi(Os^{II}) \rightarrow \pi^*(bpy,pz)$ bands in the visible. Compared to L = 4,4′-bipyridine, the $d\pi \rightarrow d\pi(Os^{III})$ bands are shifted to lower energy (5770 vs 6070 cm^{-1} for $d\pi_1 \rightarrow d\pi_3$ in CD_3CN) and are more intense (ϵ = l400 M^{-1} cm^{-1} vs 450 M^{-1} cm^{-1}).

In solvents between DN = 11.9 and 24, a structured IT band appears at 8100 ± 100 cm^{-1}. Its energy and bandwidth are only weakly solvent dependent. The structure is most clearly discernible in trimethyl phosphate and acetonitrile where the splitting between the two components is ~900 cm^{-1}.[20] Band halfwidths for the composite band ($\Delta\bar{\nu}_{1/2} = 1140-1340$ cm^{-1}) are considerably less than for L = 4,4′-bpy ($\Delta\bar{\nu}_{1/2}$ ~3800 cm^{-1} in DMSO-d_6) and molar absorptivities are greater, Table 1.

IR data are reinforcing (Figure 7 and Table 2). In CD_3CN, ν(bpy,pz) bands for Os^{III} appear at 1244 and 1317 cm^{-1} in $[(bpy)_2ClOs^{III}(pz)Ru^{II}(NH_3)_5]^{4+}$ and 1244 and 1318 cm^{-1} in $[(bpy)_2ClOs^{III}(pz)Ru^{III}(NH_3)_5]^{5+}$. Bands for Os^{II} at 1258 and 1263 cm^{-1} (sh) in $[(bpy)_2ClOs^{II}(pz)Ru^{II}(NH_3)_5]^{3+}$ disappear in the spectrum of $Os^{III}-Ru^{II}$.

The pattern of ν(bpy) bands in $[(bpy)_2ClOs^{III}(pz)Ru^{II}(NH_3)_5]^{4+}$ from 1420 to 1500 cm^{-1} resembles $Os^{III}-Ru^{III}$ with ν(bpy) bands at 1435, 1451, 1469, and 1496 cm^{-1} rather

(14) Kober, E. M.; Meyer, T. J. *Inorg. Chem.* **1983**, *22*, 1614.

(15) (a) Kober, E. M.; Goldsby, K. A.; Narayana, D. N. S.; Meyer, T. J. *J. Am. Chem. Soc.* **1983**, *105*, 4303. (b) $d\pi \rightarrow d\pi$ bands in analogous $[Os^{III}(NH_3)_5(N\text{-heterocycle})]^{3+}$ complexes have been observed at ~4750 and 5700 cm^{-1}: Lay, P. A.; Magnuson, R. H.; Taube, H. *Inorg. Chem.* **1988**, *27*, 2848.

(16) Goodman, B. A.; Raynor, J. B. *Adv. Inorg. Chem. Radiochem.* **1970**, *13*, 135.

(17) Kober, E. M.; Neyhart, G. A. Unpublished results.

(18) Creutz, C. *Prog. Inorg. Chem.* **1983**, *30*, 1.

(19) Powers, M. J.; Meyer, T. J. *J. Am. Chem. Soc.* **1980**, *102*, 1289.

(20) Similar spacing are observed in $[(NH_3)_5Ru(pz)Ru(NH_3)_5]^{5+}$, (Furholz, U.; Burgi, H. B.; Wagner, F. E.; Stabler, A.; Ammeter, J. H.; Krausz, E.; Clark, R. J. H.; Stead, M. J.; Ludi, A. *J. Am. Chem. Soc.* **1984**, *106*, 121) and $[(NH_3)_4Ru(bptz)Ru(NH_3)_4]^{5+}$ (bptz is 3,6-bis(2-pyridyl-1,2,4,5-tetrazine) (Poppe, J.; Moscherosch, M.; Kaim, W. *Inorg. Chem.* 1993, 32, 2640). In the latter there is evidence for at least three components with spacings of ~900 cm^{-1}. The structure may be vibronic in origin but it is hard to reconcile an apparent spacing of ~900 cm^{-1} given the vibrational spectrum.

Scheme 3

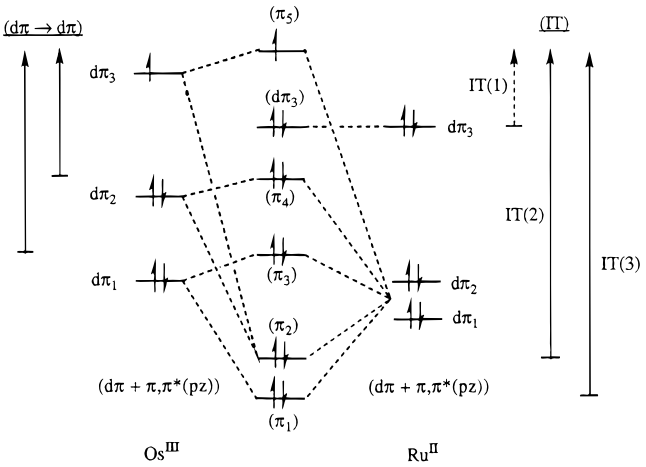

than at 1421, 1433, 1461, and 1479 cm^{-1} as in $[(bpy)_2ClOs^{II}(pz)Ru^{II}(NH_3)_5]^{3+}$.

The ν(bpy) band at 1608 cm^{-1} is intense, characteristic of Os^{III}. In $[(bpy)_2ClOs^{II}(pz)Ru^{II}(NH_3)_5]^{3+}$ it appears as a barely discernible shoulder. An intense ν(pz) stretch appears at 1599 cm^{-1} for $Os^{III}-Ru^{II}$ and at 1595 cm^{-1} for Os^{II}-Ru^{II} and is absent for $Os^{III}-Ru^{III}$. In $[(bpy)_2ClRu(pz)RuCl(bpy)_2]^{4+/3+/2+}$, ν(pz) appears only for the +3, mixed-valence ion because of the electronic asymmetry of the localized $Ru^{III}-Ru^{II}$ oxidation states.[21] Spectra in CD_3CN and KBr are the same except for minor shifts in band energies showing that the oxidation states are $Os^{III}-Ru^{II}$ in KBr as well.

Oxidation state markers in the UV−vis, NIR, and IR all point to localized Os^{III} and Ru^{II} oxidation states in $[(bpy)_2ClOs^{III}(pz)Ru^{II}(NH_3)_5]^{4+}$. There is also evidence for extensive electronic delocalization. Delocalization provides the coupling mechanism for the intensity of the remote MLCT transition in eq 1. It causes the shift to lower energy and intensity increases in the $d\pi \rightarrow d\pi(Os^{III})$ bands. It is manifested in the narrow, nearly solvent independent IT band(s) at 8000 cm^{-1}. It also appears in the electrochemistry.[1]

The NIR spectrum of $[(NH_3)_5Os(pz)Os(NH_3)_5]^{5+}$ has been analyzed by assuming complete electronic delocalization and oxidation states $Os^{II.5}-Os^{II.5}$.[22] Based on this analysis, five low-energy transitions are predicted, three of which are dipole allowed. The analysis could not be extended to $[(NH_3)_5Ru(pz)Ru(NH_3)_5]^{5+}$ which has a structured, narrow IT band at ~6400 cm^{-1} in water,[21,23] similar in shape to the IT band for $[(bpy)_2ClOs^{III}(pz)Ru^{II}(NH_3)_5]^{4+}$ at 8100 cm^{-1}.

The NIR spectrum of $[(bpy)_2ClOs^{III}(pz)Ru^{II}(NH_3)_5]^{4+}$ can be assigned based on the schematic energy level diagram in Scheme 3. In constructing the diagram, it was assumed that $d\pi(Os^{III})$ and $d\pi(Ru^{II})$ were pre-mixed with π(pz) and π*(pz). These orbitals promote $d\pi(Os^{III})-\pi(pz)-d\pi(Ru^{II})$ and $d\pi(Os^{III})-\pi^*(pz)-d\pi(Ru^{II})$ coupling across the bridge.

Taking $Os^{III}-pz-Ru^{II}$ as the z axis, $d\pi_1(Ru^{II})$ and $d\pi_2(Ru^{II})$ have considerable d_{xz}, d_{yz} character and $d\pi_3(Ru^{II})$ is largely d_{xy}. Because of the low symmetry and spin−orbit coupling at Os^{III}, the three $d\pi(Os^{III})$ orbitals all have considerable d_{xy}, d_{xz}, and d_{yz} character.[11,14] The five orbitals with *z* character mix with π(pz) and π*(pz) and couple the metals electronically.

The coupling diagram in Scheme 3 accounts for the following: (1) The increase in intensity and shift to lower energy of the $d\pi \rightarrow d\pi(Os^{III})$ bands compared to related Os(III) complexes.[11] This is caused by $d\pi(Os^{III})-d\pi(Ru^{II})$ mixing promoted by through-bridge coupling. Orbital mixing imparts charge transfer character to these normally LaPorte forbidden transitions. (2) An orbital basis for explaining the intensity of the remote CT band in eq 1. (3) The IT components at ~8100 and ~9000 cm^{-1} in CD_3CN which can be assigned to IT(2) and IT(3). In this interpretation the splitting of ~900 cm^{-1} has an electronic origin. Its magnitude is near the free ion spin−orbit coupling constant for Ru^{III} (~1250 cm^{-1}).[16] (4) IT(2) and IT(3) are nearly solvent independent because they are transitions between $d\pi$ orbitals that are highly mixed with bridge orbitals. There is little charge transfer character. This mixing also explains why the nominal charge transfer transition along the bridge, $d\pi(Ru^{II}) \rightarrow \pi^*(pz)$, is also nearly solvent independent. (5) IT(2) and IT(3) are transitions that give electronic excited states: $\pi_2^2\pi_5^1 \rightarrow \pi_2^1\pi_5^1$ (IT(2)); and $\pi_1^2\pi_5^1 \rightarrow \pi_1^1\pi_5^1$ (IT(3)). This explains why these bands appear at relatively high energies even though the underlying transitions are not coupled to the solvent.

Similar conclusions have been reached for metal-to-ligand charge transfer in $[Ru(NH_3)_5(Me\text{-}pz^+)]^{3+}$ (Me-pz^+ is *N*-methyl pyrazinium cation).

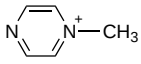

(Me-pz^+)

For this complex an intense, nearly solvent-independent band appears at 540 nm in CH_3CN.[25] The absence of a solvent dependence was explained by extensive $d\pi(Ru^{II})-\pi^*(Me\text{-}pz^+)$ mixing in the ground state and $d\pi(Ru^{III})-\pi(Me\text{-}pz^{\cdot})$ mixing in the excited state. This blends the electronic character of the donor and acceptor orbitals and diminishes the degree of charge transfer.

According to Scheme 3, there should be an additional, low energy IT band, IT(1). It would be of low intensity and have charge transfer character given its orbital origin, $d\pi_3(Ru^{II}) \rightarrow \pi_5$. Such a band does appear in the spectrum of $[Ru(NH_3)_5(Me\text{-}pz^+)]^{3+}$ (at λ_{max} = 855 nm in CH_3CN).[25] It is solvent dependent and has been assigned to $d\pi_3 \rightarrow \pi^*(Me\text{-}pz^+)$, analogous to IT(1) in Scheme 3. A low-energy band also appears in the spectrum of $[(NH_3)_5Ru(pz)Ru(NH_3)_5]^{5+}$ at ~2000 cm^{-1} (ϵ = 300 M^{-1} cm^{-1}, $\Delta\bar{\nu}_{1/2}$ ~ 1400 cm^{-1}) in D_2O.[24] Another has been reported at ~4000 cm^{-1} in nafion films and poly(vinyl alcohol) foils by MCD measurements.[26] In the spectrum of $[(bpy)_2ClOs^{III}(pz)Ru^{II}(NH_3)_5]^{4+}$ there is enhanced absorptivity near ~4000 cm^{-1} in CD_3CN, but there is no definitive evidence for a new band attributable to IT(1). If it appears at lower energy in the IR it must be of low absorptivity (ϵ < 500 M^{-1} cm^{-1}).

The model depicted in Scheme 3 differs from three-center models used in the literature to describe $[(NH_3)_5Ru(pz)Ru(NH_3)_5]^{5+}$.[27−29] In those models the 4d orbitals at each Ru are hybridized to give two orbitals which are involved in σ bonding, one $d\pi$ orbital in the *xy* plane orthogonal to π,π*(pz), one $d\pi$ orbital having *z* character but orthogonal to π,π*(pz),

(21) Callahan, R. W.; Keene, F. R.; Meyer, T. J. *J. Am. Chem. Soc.* **1977**, *99*, 1064.
(22) (a) Dubicki, L.; Ferguson, J; Krausz, E. R. *J. Am. Chem. Soc.* **1985**, *105*, 2507. (b) Dubicki, L.; Ferguson, J.; Krausz, E. R.; Lay, P. A.; Maeder, M.; Magnuson, R.; Taube, H. *J. Am. Chem. Soc.* **1985**, *107*, 2167.
(23) Creutz, C.; Taube, H. *J. Am. Chem. Soc.* **1973**, *95*, 1086.
(24) Best, S. P.; Clark, R. J. H.; McQueen, R. C. S.; Joss, S. *J. Am. Chem. Soc.* **1989**, *111*, 548.
(25) Creutz, C.; Chou, M. H. *Inorg. Chem.* **1987**, *26*, 2995.
(26) (a) Krausz, E. *Chem. Phys. Lett.* **1985**, *120*, 113. (b) Krausz, E.; Ludi, A. *Inorg. Chem.* **1985**, *24*, 939.
(27) Piepho, S. B. *J. Am. Chem. Soc.* **1990**, *112*, 4197.
(28) (a) Zhang, L.-T.; Ko, J.; Ondrechen, M. J. *J. Am. Chem. Soc.* **1987**, *109*, 1666. (b) Ondrechen, M. J.; Ko, J.; Zhang, L.-T. *J. Am. Chem. Soc.* **1987**, *109*, 1672. (c) Zhang, L.-T.; Ko, J.; Ondrechen, M. J. *J. Phys. Chem.* **1989**, *93*, 3030.
(29) Broo, A.; Larsson, S. *Chem. Phys.* **1992**, *161*, 363.

and one dπ orbital having *z* character with appropriate symmetry for overlap with π,π^*(pz). Gerade and ungerade combinations of the z-axis d orbitals mix with π,π^*(pz) orbitals of appropriate symmetry. In this coupling scheme, the plane of the pyrazine ligand is assumed to coincide with one of the z-axis octahedral planes at each of the metals.

The unsymmetrical nature of $[(bpy)_2ClOs^{III}(pz)Ru^{II}(NH_3)_5]^{4+}$ complicates the description of electronic structure. The model in Scheme 3 assumes that dπ_1, dπ_2, and dπ_3 at Os^{III} all have considerable d_{xy}, d_{xz}, and d_{yz} character because of the low symmetry at the metal and spin−orbit coupling.[11,14] All three are mixed with π(pz) and π^*(pz). This provides an orbital mechanism for delocalization by mixing these orbitals with ligand-mixed orbitals of appropriate symmetry at ruthenium.

At ruthenium, the three dπ orbitals are more closely represented by d_{xz}, d_{xz} (dπ_1, dπ_2), and d_{xy} (dπ_3). The two orbitals with *z* character mix with π(pz) and π^*(pz). The remaining orbital is orthogonal to the Os^{III}(pz)Ru^{II} interaction and weakly coupled to Os^{III}. d_{xz} (dπ_1) and d_{yz} (dπ_2) lie at lower energy because of extensive mixing with π^*(pz).

Scheme 3 provides an electronic interpretation for the structured IT band. For $[(NH_3)_5Ru(pz)Ru(NH_3)_5]^{5+}$,[27−29] the structure in the analogous NIR band has been assumed to be vibronic with a single electronic origin. In comparing Scheme 3 to the three center models, other properties do not depend on whether one or two dπ(Ru) orbitals are strongly mixed with dπ(Os).

Scheme 3 also provides an electronic interpretation for how there can be extensive delocalization *and* localized oxidation states. As for $[(NH_3)_5Ru(pz)Ru(NH_3)_5]^{5+}$, the intense NIR band(s) for $[(bpy)_2ClOs^{III}(pz)Ru^{II}(NH_3)_5]^{4+}$ are electronic transitions between orbitals that are strongly coupled through the bridge. Nonetheless, the highest filled level is $d_{xy}(Ru^{II})$ and it is only slightly mixed with π,π^*(pz). There is no counterpart to this orbital at osmium. All three d$\pi(Os^{III})$ orbitals are coupled to π,π^*(pz). Thus, the apparent ambiguity of strong electronic coupling and localized oxidation states occurs as a natural consequence of the symmetry imposed by the bridge and differences in π,π^*(pz) mixing between dπ_1, d$\pi_2(Ru^{II})$, and d$\pi_3(Ru^{II})$. Localization is a consequence of weak electronic coupling to d$\pi_3(Ru^{II})$ and residual coupling to intramolecular vibrations and the solvent which create a barrier to electron transfer.

There is a difference in electronic structure in $[(NH_3)_5Ru(pz)Ru(NH_3)_5]^{5+}$ because of the increase in symmetry. The odd electron may be evenly distributed between the metals as is usually assumed,[27−29] consistent with electronic Stark effect measurements.[30] The results of resonance Raman studies on the NIR band demonstrate that ν(pz) vibrations are coupled to the underlying transitions, consistent with through-bridge coupling.[31] If residual localization exists, it could be explained by a modified form of Scheme 3. Strong through-bridge $d_{xz},d_{yz}-\pi,\pi^*(pz)-d_{xz},d_{yz}$ coupling would exist across the bridge with the NIR band(s) arising from the analogs of IT(2) and IT(3) in Scheme 3. As in $[(bpy)_2ClOs^{III}(pz)Ru^{II}(NH_3)_5]^{4+}$ residual localization exists because $d_{xy}(Ru^{II})$ is the highest filled level and only slightly mixed with π,π^*(pz). Measurements on the IT band at ~6400 cm^{-1} are not directly relevant to the question of localization or delocalization of oxidation states. Localization would be a consequence of weak electronic coupling and a residual barrier to electron transfer from the solvent and intramolecular vibrations.

In $[(bpy)_2ClOs^{III}(pz)Ru^{II}(NH_3)_5]^{4+}$ in nitromethane and nitrobenzene there may be a greater degree of localization imparting charge transfer character to IT(2) and IT(3). In these solvents the IT band is solvent dependent, shifts to higher energy (by ~1000 cm^{-1}), and increases in bandwidth (Figure 4, Table 1). These are solvents of low donor number where the difference between $E_{1/2}(Os^{III/II})$ and $E_{1/2}(Ru^{III/II})$ is greatest.[1] This enhances redox asymmetry and decreases d$\pi-\pi,\pi^*$(pz)−dπ coupling and the extent of delocalization.

Mixed-Valence Isomers. Intramolecular Electron Transfer. In formamide (DN = 24.0) IT(1) appears at 5900 cm^{-1} for $[(bpy)_2ClOs^{II}(pz)Ru^{III}(NH_3)_5]^{4+}$. A second band appears at 8020 cm^{-1}. It has the energy and bandshape of IT(2), IT(3) in $[(bpy)_2ClOs^{III}(pz)Ru^{II}(NH_3)_5]^{4+}$. This provides evidence for the equilibrium in eq 3, with $Os^{II}-Ru^{III}$ dominant based on the relative intensities of the bands.

$$[(bpy)_2ClOs^{III}(pz)Ru^{II}(NH_3)_5]^{4+} \rightleftharpoons [(bpy)_2ClOs^{II}(pz)Ru^{III}(NH_3)_5]^{4+} \quad (3)$$

The equilibrium is temperature dependent in trimethyl phosphate (DN = 23.0), Figure 6, with an equilibrium constant $K = [Os^{II}-Ru^{III}]/[Os^{III}-Ru^{II}] = 1.1$ (316 K), 2.8 (297 K), and 9.0 (274 K).[32] From the relationship, $\ln K = (-\Delta H°/RT) + \Delta S°/R$ (inset, Figure 6), $\Delta H° = -8.2 \pm 2$ kcal/mol and $\Delta S° = -27 \pm 6$ eu. The entropic change is within experimental error of $\Delta S°$ (=−21 ± 6 eu) for the analogous Ru−Ru complex measured electrochemically, eq 4.[33]

$$[(bpy)_2ClRu^{III}(pz)Ru^{II}(NH_3)_5]^{4+} \rightarrow [(bpy)_2ClRu^{II}(pz)Ru^{III}(NH_3)_5]^{4+} \quad (4)$$

$\Delta S°$ is unfavorable largely due to the increase in solvent polarization at $-Ru^{III}(NH_3)_5^{3+}$ compared to $-Ru^{II}(NH_3)_5^{2+}$, which increases electrostriction in the surrounding solvent.

The isomers $[(bpy)_2ClOs^{II}(pz)Ru^{III}(NH_3)_5]^{4+}$ and $[(bpy)_2ClOs^{III}(pz)Ru^{II}(NH_3)_5]^{4+}$ coexist in formamide and trimethyl phosphate even though they differ in internal electronic structure, in particular in the extent of through-bridge electronic coupling. This is an interesting case where the internal electronic structure of the ion is strongly coupled to the solvent. The role of the solvent can be explained by invoking differences in H-bonding interactions between $-Ru^{III}(NH_3)_5^{3+}$ and $-Ru^{II}(NH_3)_5^{2+}$ and the effect this has on d$\pi-\pi,\pi^*$(pz) mixing.[1]

Optical electron transfer in $[(bpy)_2ClOs^{II}(pz)Ru^{III}(NH_3)_5]^{4+}$ results in instantaneous formation of a Franck−Condon state "$[(bpy)_2ClOs^{III}(pz)Ru^{II}(NH_3)_5]^{4+}$" which has the electronic configuration $Os^{III}-Ru^{II}$ but the nuclear coordinates of Os^{II}-Ru^{III}. Relaxation follows with the vibrations and surrounding solvent adjusting to the change from $Os^{II}-Ru^{III}$ to $Os^{III}-Ru^{II}$. *Relaxation of the solvent is accompanied by a change in internal electronic structure.* As the solvent relaxes, through-bridge electronic coupling increases. This increases the electronic delocalization energy, H_{ab}, with $H_{ab}(Os^{II}-Ru^{III}) < H_{ab}(Os^{III}-Ru^{II})$ and H_{ab} taken as a positive quantity.

The opposite is true for $[(bpy)_2ClOs^{III}(pz)Ru^{II}(NH_3)_5]^{4+}$. Excitation to "$[(bpy)_2ClOs^{II}(pz)Ru^{III}(NH_3)_5]^{4+}$" is followed by solvent relaxation and a decrease in electronic coupling from $H_{ab}(Os^{III}-Ru^{II})$ to $H_{ab}(Os^{II}-Ru^{III})$. There is no simple relation-

(30) Oh, D. H.; Sano, M.; Boxer, S. G. *J. Am. Chem. Soc.* **1991**, *113*, 6880.

(31) Petrov, V.; Hupp, J. T.; Mottley, C.; Mann, L. C. *J. Am. Chem. Soc.* **1994**, *116*, 2171.

(32) Equilibrium constants (*K*) were calculated by using averaged ϵ values in Table 3: ϵ(6000 cm^{-1}) = 600 M^{-1} cm^{-1}, ϵ(8100 cm^{-1}) = 470 M^{-1} cm^{-1} for $Os^{II}-Ru^{III}$; ϵ(6000 cm^{-1}) = 850 $M^{-1}cm^{-1}$, ϵ(8100 cm^{-1}) = 1800 M^{-1} cm^{-1} for $Os^{III}-Ru^{II}$.

(33) Hupp, J. T.; Neyhart, G. A.; Meyer, T. J.; Kober, E. M. *J. Phys. Chem.* **1992**, *96*, 10820.

ship between optical and thermal electron transfer. The equations derived by Hush for IT bands, which relate E_{op}, $\Delta G°$, and the reorganizational energy (λ), all assume the validity of the Condon approximation.[34]

The low-energy orbital pathway for $Os^{II} \rightarrow Ru^{III}$ thermal electron transfer in $[(bpy)_2ClOs^{II}(pz)Ru^{III}(NH_3)_5]^{4+}$ is $d\pi_3(Os^{II}) \rightarrow d\pi_3(Ru^{III})$. The other pathways, $d\pi_1,d\pi_2(Os^{II}) \rightarrow d\pi_3(Ru^{III})$, give interconfigurational excited states at Os^{III}, $(d\pi_1)^2,(d\pi_2)^1,(d\pi_3)^2$ or $(d\pi_1)^1,(d\pi_2)^2,(d\pi_3)^2$, as products. These are high-energy pathways and do not contribute appreciably at room temperature. Because of the change in H_{ab} between $Os^{III}-Ru^{II}$ and $Os^{II}-Ru^{III}$, the thermal barrier to $Os^{II} \rightarrow Ru^{III}$ electron transfer is defined by the usual vibrational and collective solvent coordinates but electronic coordinates are coupled into the transition as well.[27,36,37]

An estimate of $H_{ab}(Os^{II}-Ru^{III})$ for $[(bpy)_2ClOs^{II}(pz)Ru^{III}(NH_3)_5]^{4+}$ can be made based on eq 5 and the properties of the IT band.[34] In eq 5, ϵ_{max} is the molar extinction coefficient

$$H_{ab} = ((4.2 \times 10^{-4})\epsilon_{max}\Delta\bar{\nu}_{1/2}E_{op}/d^2)^{1/2} \qquad (5)$$

at the maximum in M^{-1} cm^{-1}, $\Delta\bar{\nu}_{1/2}$ is the bandwidth at half height in cm^{-1}, E_{op} is the absorption maximum in cm^{-1}, and d is the metal−metal separation distance in angstroms (d = 6.9 Å for L = pz). In dimethyl sulfoxide $H_{ab}(Os^{II}-Ru^{III}) = 325$ cm^{-1}. This is probably a lower limit. In related complexes it has been found that the actual charge transfer distance is less than the geometrical distance.[35]

$H_{ab}(Os^{II}-Ru^{III})$ is the *sum* of separate resonance energies from $d\pi_3(Os^{II})-d\pi_3(Ru^{III})$, $d\pi_2(Os^{II})-d\pi_3(Ru^{III})$, and $d\pi_1(Os^{II})-d\pi_3(Ru^{III})$ coupling across the bridge. The IT "band" is a convolution of the three transitions illustrated in Scheme 2, $d\pi_3(Os^{II}) \rightarrow d\pi_3(Ru^{III})$, $d\pi_2(Os^{II}) \rightarrow d\pi_3(Ru^{III})$, and $d\pi_1(Os^{II}) \rightarrow d\pi_3(Ru^{III})$. Further, $H_{ab}(Os^{II}-Ru^{III})$ is a measure of the mixing of $Os^{II}-Ru^{III}$ with $Os^{III}-Ru^{II}$ *but with* $Os^{III}-Ru^{II}$ *having the solvent polarization of* $Os^{II}-Ru^{III}$.

Thermal electron transfer in $[(bpy)_2ClOs^{III}(pz)Ru^{II}(NH_3)_5]^{4+}$ occurs by the pathway $d\pi_3^2\pi_5^1 \rightarrow d\pi_3^1\pi_5^2$, note Scheme 3. The pathways $\pi_1^2\pi_5^1 \rightarrow \pi_1^1\pi_5^2$ and $\pi_2^2\pi_5^1 \rightarrow \pi_2^1\pi_5^2$ give interconfigurational excited states highly mixed with π,π^*(pz). Based on the conclusion that there are localized oxidation states, there must be a residual vibrational and librational barrier to electron transfer, greatly reduced by through-pyrazine coupling. $Os^{III} \leftarrow Ru^{II}$ electron transfer is accompanied by changes in librational, vibrational, and electronic coordinates with through-bridge electronic coupling decreasing as the reaction proceeds.

$[(bpy)_2ClOs(pz)Ru(NH_3)_5]^{4+}$. Conclusions. The properties of $[(bpy)_2ClOs^{III}(pz)Ru^{II}(NH_3)_5]^{4+}$ are unusual, but not unique. It appears to be one of a number of molecules with properties at the Class II−Class III interface in the Robin and Day classification scheme.[38] The Creutz−Taube ion has similar properties.[21,24,26] In [(fulvalenyl)$Mn_2(CO)_4(\mu$-dppm)]$^+$ (dppm = $Ph_2PCH_2PPh_2$) there are ν(CO) bands in the IR for both Mn^I and Mn^{II} but $\Delta(\nu(CO))$ is small compared to isolated monomers due to electronic delocalization.[39] The mixed-valence complexes $[(P^iPr_3)_2(CO)_3M]_2(\mu$-pz)$^+$ (M = Mo, W) appear to be delocalized on the vibrational time scale based on the pattern of ν(CO) bands.[40] NIR bands are narrow and nearly solvent independent in both cases.

One key to the sometimes ambiguous properties of these ions is in the electronic symmetry created by the metal−ligand−metal bridge. Strong through-bridge coupling exists for the $d\pi$ orbitals lying along the bridge (z) axis but, for the first and second row transition metals, weak coupling exists for the $d\pi$ orbitals in the xy plane.

The internal electronic structures of the mixed-valence ions $[(bpy)_2ClOs(L)Ru(NH_3)_5]^{4+}$ (L = pz, 4,4′-bpy) are strongly coupled to the solvent. Changes in solvent can induce intramolecular electron transfer. More dramatic is the role of solvent in influencing internal electronic structure and the extent of electronic delocalization in $Os^{III}-Ru^{II}$ compared to $Os^{II}-Ru^{III}$ in the isomers of $[(bpy)_2ClOs(pz)Ru(NH_3)_5]^{4+}$.

These examples at the Class II−Class III interface raise the level of complexity of recognized mixed-valence behavior. They point to the important roles that symmetry and electronic coupling with the solvent can play. They pose new problems for theoretical investigation. Additional phenomena may remain to be observed. There could be a range of behaviors at the Class II−III interface involving subtle differences in the extent of charge transfer and even dynamical effects in the coupled vibrations or solvent librations.

Acknowledgments are made to the National Science Foundation under Grant No. CHE-8503092, to the Army Research Office under Grant Nos. DAALO3-88-K-0192 and DAALO3-92-G-0198 for support of this research, and to Joe Hupp for initial results and helpful discussion.

Supporting Information Available: Tables of near-UV−visible band energies as a function of solvent for $[(bpy)_2ClOs^{II}(L)Ru^{II}(NH_3)_5]^{3+}$, of selected UV−visible spectral features for $[(bpy)_2ClOs(L)Ru(NH_3)_5]^{4+}$ as a function of solvent, of selected features in the IR spectra of $[(bpy)_2ClOs(L)Ru(NH_3)_5]^{5+/4+/3+}$ (L = pz, 4,4′-bpy), and a figure of the IR spectra of $[Os(bpy)_2(pz)Cl]^+$ and $[Os(bpy)_2(pz)Cl]^{2+}$ in CD_3CN (5 pages). This material is contained in many libraries on microfiche, immediately follows this article in the microfilm version of the journal, can be ordered from the ACS, and can be downloaded from the Internet; see any current masthead page for ordering information and Internet access instructions.

JA9535672

(34) (a) Hush, N. S. *Prog. Inorg. Chem.* **1967**, *8*, 391. (b) Hush, N. S. *Electrochim. Acta* **1968**, *13*, 1005.

(35) Hupp, J. T.; Dong, Y.; Blackburn, R. L.; Lu, H. *J. Phys. Chem.* **1993**, *97* 3278.

(36) (a) Piepho, S. B.; Krausz, E. R.; Schatz, P. N. *J. Am. Chem. Soc.* **1978**, *100*, 2996. (b) Neuenschwander, K.; Piepho, S. B.; Schatz, P. N. *J. Am. Chem. Soc.* **1985**, *107*, 7862. (c) Prassides, K.; Schatz, P. N. *J. Phys. Chem.* **1989**, *93*, 83.

(37) Wong, K. Y.; Schatz, P. N. In *Mechanistic Aspects of Inorganic Reactions*; ACS Symposium Series, No. 198, Rorabacher, D. B., Endicott, J. F., Eds.; American Chemical Society: Washington, DC, 1982.

(38) Robin, M. B.; Day, P. *Adv. Inorg. Chem. Radiochem.* **1967**, *10*, 247.

(39) Atwood, C. G.; Geiger, W. E.; Rheingold, A. L. *J. Am. Chem. Soc.* **1993**, *115*, 5310.

(40) Bruns, W.; Kaim, W.; Waldhor, E.; Krejcik, M. *Inorg. Chem.* **1995**, *34*, 663.